2024 European Control Conference (ECC)
June 25-28, 2024. Stockholm, Sweden

Reliability-aware Control of Power Converters in Mobility Applications

Amin Rezaeizadeh[1], Gioele Zardini[2], Emilio Frazzoli[3], Silvia Mastellone[1]

***Abstract*— The large scale adoption of Battery Electric Vehicles (BEVs) is still limited by cost, reliability and lifetime considerations. The power converters of a BEVs, and more specifically the semiconductor switching devices, are the second most likely component to fail due to the damage caused by the current-induced temperature cycling. In this paper we address the active mitigation of damage in e-mobility power converters, by introducing a novel frequency-domain speed controller for the power train that reduces the thermal stress on the power electronic Insulate Gate Bipolar Transistors (IGBTs), while simultaneously ensuring effective speed tracking performance. We integrate the multi-objective problem in an $\mathcal{H}_\infty$ control framework, which embeds the semiconductor reliability model in the weights functions. The method is tested using standardised driving cycles in two different scenarios: reliability-aware, and performance-oriented cases. Finally a lifetime analysis of the IGBTs, in both scenarios is performed leveraging the Rainflow algorithm and temperature data.**

I. Introduction

BEVs hold the potential for a sustainable alternative to traditional Internal Combustion Engine Vehicles (ICEVs). Today, major automotive manufacturers such as Toyota, Mitsubishi, Ford, Renault, and Nissan are transitioning towards full-electric vehicle lineups. Together with the scientific and technical communities, they face the challenge of advancing the power conversion technology required for enabling the transition towards the next generation of BEVs. These power converters are expected to reduce CO_2 emissions (e.g., when considering tank-to-wheel performance), enhance energy efficiency, and boost reliability for a wide range of BEVs and Hybrid Electric Vehicles (HEVs) while maintaining affordability to encourage widespread BEV adoption [1]–[4]. These challenges become even more critical when considering future Autonomous Mobility-on-Demand (AMoD) services utilizing BEVs, as they demand significant computational and energy resources [5, 6].

Despite their numerous advantages, electric vehicles still fall short in terms of reliability and longevity compared to their combustion engine counterparts. Addressing these sustainability issues is the primary focus of this work.

Conventionally electric vehicles are designed and operated to optimize performance and efficiency. Reliability aspects are considered in order to assesses a system's ability to withstand failures over time, estimates its expected lifespan, and predicts time-to-failure [7]- [8]. This information is used to design components, to plan maintenance and replacements, but it is not considered during the operation phase. However, responsible system operation contributes to minimize long-term damage and increase the system's lifespan by utilizing reliability information about components, systems, and fleets. In this research, we apply the concept of *reliability control* to electric vehicle power converters, where the converter's operation is optimized to minimize damage and maximize the vehicle's lifetime and availability.

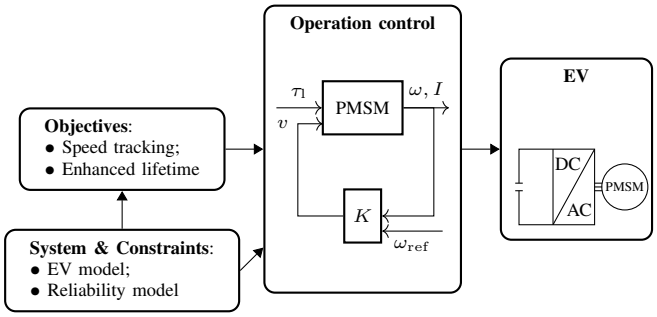

Fig. 1: $\mathcal{H}_\infty$ control scheme to operate a BEV integrating vehicle and reliability models. Control objectives are speed tracking and enhanced lifetime of the vehicle.

Our focus is on an automotive power converter that uses standard Silicon Insulated-Gate Bipolar Transistor (IGBT) technology.

Those devices are the technology at the core of BEV drivetrain [9, 10], they drive the motors enabling power conditioning and adaptation to driving requirements across a wide range of conditions [11]. However, they are also identified as the component most likely to fail after the battery pack [12]. The performance of a power converter depends, to a large extent, on the control of its semiconductor switches under various applications and electrical loads. Properly optimizing their operation can lead to increase the lifespan for the whole converter. Reliability of power semiconductor devices is typically studied [13]–[18], for analysis purpose in lifetime prediction applications using well established, empirically-based damage models.

In our research, we employ reliability models to design an $\mathcal{H}_\infty$ controller that operates the BEV power converter *efficiently* and *reliably* for each driving cycle and operating condition (see Fig.1).

While reliability studies typically are dedicated to observe

[1]Institute of Electric Power Systems, University of Applied Science Northwest Switzerland, Windish, Switzerland, {amin.rezaeizadeh,silvia.mastellone}@fhnw.ch

[2]Laboratory for Information and Decision Systems, Massachusetts Institute of Technology, Cambridge, MA 02139, USA gzardini@mit.edu.

[3]Institute for Dynamic Systems and Control, ETH Zürich, Switzerland efrazzoli@ethz.ch.

This work was supported by the Swiss National Science Foundation under NCCR Automation, grant agreement 51NF40_180545, and by the Swiss Federal Office of Energy (SFOE).

and characterize system longevity and failure resistance, we propose a reliability control approach to actively operate the system to increase its resistance to failure. This is achieved by integrating reliability objectives into a multi-objective optimization control problem, such that the performance and degradation aspects of system operation are balanced.

The control policies are then tested on realistic case studies, where standard drive cycles are used as vehicle desired speed profiles. The resulting trajectories and damage accumulation are compared a-posteriori in various scenarios to assess the energy efficiency and lifetime performance. The paper is structured as follows: Section II describes the automotive power train, its mathematical models and states the control design problem. Section III introduces models for sustainability metrics, it details the semiconductor characteristics and its losses and damage models used to estimate the device efficiency and reliability. Section IV presents the main result, the $\mathcal{H}_\infty$ controller, whose performance results are validated in Section V. Section VI is dedicated to concluding remarks and future research directions.

II. Problem Statement

This paper considers an BEVs powertrain consisting of a battery supplying power to a three-phase voltage source converter, which controls the operation of Permanent Magnet Synchronous Motors (PMSMs), as shown in Figure 2. The rotor angle, θ, measured by an encoder is used to estimate the mechanical speed, ω_m and in the Park dq0-transformation [19] to rotate the reference frames of the AC current waveforms such that they become DC signals. The reference speed, ω_{ref}, ω_m and the dq-components of the motor current, i_d and i_q, are used by the controller $K(s)$ to design the desired d- and q-components of the stator voltage, i.e. u_d and u_q, respectively. Using Park's inverse transformation, these values are converted back to the static coordinate frame where the Space vector Pulse Width Modulation (SVPWM) determine the switching patterns required to produce the desired voltage.

In the family of electric motors for mobility applications, PMSM are characterized by high power density, stable output torque, low noise, and good speed regulation performance, making them suitable for EV propulsion [20]–[22]. A mathematical model of PMSMs is described in the d-q reference frame by:

$$u_d(t) = R_{\text{s}} i_d(t) + L_d \frac{\partial i_d(t)}{\partial t} - \omega_{\text{e}} L_q i_q(t), \tag{1}$$

$$u_q(t) = R_{\text{s}} i_q(t) + L_q \frac{\partial i_q(t)}{\partial t} + \omega_{\text{e}} L_d i_d(t) + \omega_{\text{e}} \Phi_{\text{F}}, \tag{2}$$

where R_{s} is the stator resistance, L_d and L_q are d-axis and q-axis inductances, ω_{e} is the rotational speed of the electrical field and Φ_{F} is the magnetic flux of the permanent magnet which we assume to be constant. Moreover, the induced EMF is assumed to be sinusoidal and hysteresis and eddy currents loss are neglected.

The produced electrical torque is given by:

$$\tau_{\text{e}} = \frac{3}{2} p \Phi_{\text{F}} i_q(t) + \frac{3}{2} p (L_d - L_q) i_d(t) i_q(t), \tag{3}$$

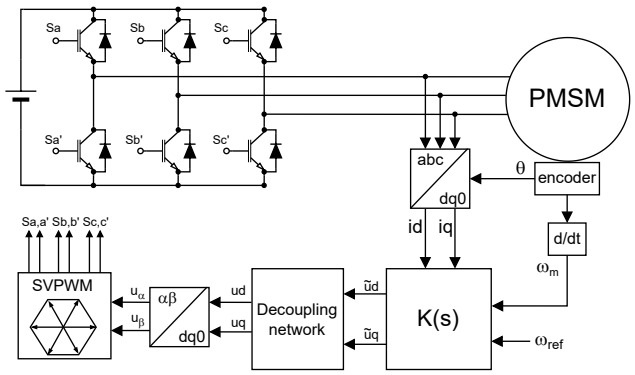

Fig. 2: The PMSM system drive with speed tracking and IGBT semiconductors reliability control scheme.

where p is the number of pole pairs. The rotor mechanical speed is governed by the following inertial equation:

$$\tau_{\text{e}} - \tau_{\text{l}} = J \frac{\partial \omega_{\text{m}}(t)}{\partial t} + B_{\text{f}} \omega_{\text{m}}(t), \tag{4}$$

where τ_{l} denotes the load torque, J is the moment of inertia, B_{f} is the viscous friction coefficient, and $\omega_{\text{m}} = \omega_{\text{e}}/p$ is the rotor mechanical speed.

The control objective is to design a suitable stator voltage to control the current and produce the torque required to track the reference speed, while minimizing converter losses and damage. The motor dynamics described above include bi-linear terms, to linearize those dynamics we define the following auxiliary control inputs:

$$\tilde{u}_d(t) \coloneqq u_d(t) + \omega_{\text{e}} L_q i_q(t), \tag{5}$$

$$\tilde{u}_q(t) \coloneqq u_q(t) - \omega_{\text{e}} L_d i_d(t) - \omega_{\text{e}} \Phi_{\text{F}}. \tag{6}$$

With these auxiliary control variables, the PMSM voltage equations become linear:

$$L_d \frac{\partial i_d(t)}{\partial t} \coloneqq \tilde{u}_d(t) - R_{\text{s}} i_d(t), \tag{7}$$

$$L_q \frac{\partial i_q(t)}{\partial t} \coloneqq \tilde{u}_q(t) - R_{\text{s}} i_q(t). \tag{8}$$

Furthermore, we consider a surface-mounted type of PMSM where $L_d \approx L_q$, and neglect the reluctance torque term, so the speed equation becomes linear:

$$J \frac{\partial \omega_{\text{m}}(t)}{\partial t} = \frac{3}{2} p \Phi_{\text{F}} i_q(t) - \tau_{\text{l}} - B_{\text{f}} \omega_{\text{m}}(t), \tag{9}$$

Once the required $\tilde{u}_d(t)$, $\tilde{u}_q(t)$ are determined by the controller, the actual desired stator voltage is then calculated as:

$$u_d(t) = \tilde{u}_d(t) - \omega_{\text{e}} L_q i_q(t), \tag{10}$$

$$u_q(t) = \tilde{u}_q(t) + \omega_{\text{e}} L_d i_d(t) + \omega_{\text{e}} \Phi_{\text{F}}, \tag{11}$$

assuming precise measurement of ω_{m}, and knowledge of motor parameters Φ_{F}, L_d and L_q. The notation $\tilde{\cdot}$ is omitted in the following for the sake of brevity.

III. Modeling and Responsibility Metrics

To include efficiency and reliability requirements in the control design, we need to define damage models that enable us to estimate the health status of the converter semiconductor components. These serve as basis to define responsibility metrics that determine how components, and systems should be operated. Starting from individual components, we use mathematical reliability models to estimate the damage experienced as a function of the environmental and operating conditions. Here we focus on bond wire fatigue, as it is one of the dominant failure modes in IGBT modules under cyclic stresses. Specifically, in a power BEV converter energy losses and damage can be modeled as a function of the current and therefore of the driving conditions [23, 24]. In a second step, we consider physically interconnected components in a system and define new resulting estimates of reliability for the whole converter based on the drive-cycles and operation.

Once we have defined models and measures for reliability, we can proceed to integrate sustainability objectives in the control design process.

A. Lifetime model of IGBTs

A major reason for the failure of IGBTs in power converters is bond wire lift-off and stress cracks which links the various components of the IGBT [16]–[18, 25]. Such damage is due to the recurring thermal fluctuations experienced by the device during its operation. As the device's junction temperature fluctuates, the discrepancy in the thermal expansion properties between the two materials results in stress at the bonding interface between the wire and the silicon. Consequently, the bond wires become disconnected, leading to an open-circuit failure.

The number of cycles to failure can be anticipated based on a specific lifetime model.

In this study, we use the following empirical lifetime model for IGBT modules [26]:

$$N_{\mathrm{f}} = A_0 . A_1^{\beta} . \Delta T_j^{\alpha-\beta} . \exp\left(\frac{E_{\mathrm{a}}}{\kappa_{\mathrm{B}} T_j}\right) . \frac{C + {t_{on}}^{\gamma}}{C + 2^{\gamma}} . k_{\mathrm{thick}}, \tag{12}$$

with

$$\beta = \exp \frac{-(\Delta T_j - T_0)}{\lambda},$$

where N_{f} is the number of cycles to failure which is inversely dependent on several factors, including the medium junction temperature, T_j, the magnitude of the temperature cycle, ΔT_j, and the duration of the cycle, t_{on}. The remaining factors are constant parameters: E_{a} and κ_{B} are, respectively, the activation energy and the Boltzmann constant, k_{thick} is the chip thickness factor, and A_0, A_1, T_0, λ, α, C, γ are constants empirically determined by the semiconductor device manufacturer.

Using standard values detailed in the components datasheet [26], we observe an inverse relation between the magnitude of the temperature fluctuation and the number of cycles to failure. For example, when an IGBT is subjected to a temperature stress of $\Delta T_j = 40^{\circ}$ in the process, it can endure approximately 922k cycles at the average junction temperature of $T_j = 150^{\circ}$ and duration of $t_{\mathrm{on}} = 10s$. However, at the same temperature and cycle duration but with a higher temperature stress of $\Delta T_j = 80^{\circ}$, the expected number of cycles is only about 30k. It can also be observed that as the duration of temperature cycles t_{on} increases, the number of cycles to failure slightly decreases.

B. Thermal model of junction temperature

The IGBT junction temperature T_{j} and its fluctuation ΔT_{j} can be simulated using a first order thermal model [27]:

$$C_\theta \dot{T_{\mathrm{j}}}(t) = P(t) - \frac{T_{\mathrm{j}}(t) - T_{\mathrm{a}}}{R_\theta}, \tag{13}$$

where $P(t)$ denotes the power dissipated by the IGBT, T_{a} is the ambient (heatsink) temperature, and R_θ and C_θ are, respectively, the thermal resistance and capacitance of the IGBT specified in the datasheet.

For simplicity, we study only the impact of the conduction loss on the IGBT junction temperature. The conduction loss is computed by multiplying the on-state conducting current and the voltage scaled by the duty factor:

$$P(t) \approx V_{\mathrm{ce0}} I_{\mathrm{on}}(t) + r_{\mathrm{CE}} I_{\mathrm{on}}^2(t), \tag{14}$$

where V_{ce0} is the Collector-Emitter on-state voltage threshold, r_{CE} is the on-state resistance, and I_{on} denotes the on-state current.

IV. Control Design

Equipped with the electro-mechanical system, the efficiency and the reliability models, we can now proceed to design the controller. The control objective is to optimize the speed tracking, while minimizing power losses, functions of the current, and maximising the semiconductors lifetime, function of the average junction temperature and its variation. We propose a frequency domain approach, where accumulation of damage as function of thermal cycling can be captured best. We specify the performance and reliability requirements in frequency domain as weighting transfer functions, and the controller is designed through a one step linear matrix inequality (LMI) optimization.

Mathematically, the closed-loop system can be represented as

$$z = F_\ell(P(s), K(s))w, \tag{15}$$

where $F_\ell(P(s), K(s))$ denotes the lower linear fractional transformation of plant $P(s)$ closed by controller $K(s)$, w is the exogenous input which includes reference speed profiles and load torque, and z represent error signals which we want to minimize:

$$w = \begin{bmatrix} \omega_{\mathrm{ref}} \\ \tau_{\mathrm{l}} \end{bmatrix}, \quad z = \begin{bmatrix} W_e(s) e_{\mathrm{track}} \\ W_I(s) i_q \\ W_I(s) i_d \end{bmatrix},$$

where W_e and W_I are, respectively, frequency dependent weights on speed tracking error and current consumption, and e_{track} is the speed error signal.

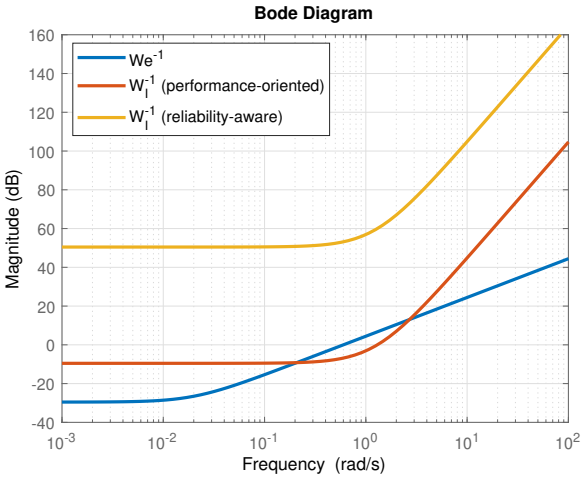

Fig. 3: Weights on the current consumption profile and tracking error in the frequency domain.

The control design objective is to minimize the $\mathcal{H}_\infty$ norm of the closed-loop transfer function from w to z, defined as:

$$\|F_\ell(P,K)\|_\infty = \sup_\omega \bar{\sigma}(F_\ell(P,K)(j\omega)), \tag{16}$$

where $\bar{\sigma}$ denotes the maximum singular value operator.

Figure 3 depicts the weight transfer functions used to design the $\mathcal{H}_\infty$ controller. $W_e(j\omega)$ is the weight penalizing the speed tracking error at all frequencies. For the given thermal model time constant $R_\theta C_\theta$, as the frequency of the current fluctuation increases, the impact on the temperature on damage decreases. Therefore, to lower the thermal stress experienced by the IGBTs, the weight on the current, W_I, is chosen as a first-order transfer function to penalize current and therefore temperature oscillations particularly in the frequency range below the thermal response bandwidth.

In the following, we compare two control modes: one with lower penalty on current consumption which results in a *Performance-Oriented* controller, and the other with significant importance on the current profile that leads to a *Reliability-Aware* control policy. Figure 2 illustrates the closed-loop system. The inputs u_d and u_q are the auxiliary inputs defined previously in Equations (5) and (6), and the controller output is modified by adding a decoupling module according to Equations (10) and (11).

V. Simulation Results

Standardized drive cycles are examples of real-world driving conditions and are frequently employed by vehicle manufacturers to determine fuel efficiency and emissions for their vehicles. Specifically, the Worldwide harmonized Light vehicles Test Cycles (WLTC) represent a series of chassis dynamometer tests specifically designed to measure CO_2 emissions and fuel consumption in light-duty vehicles.

They are a suitable testing framework for comparing the performance of different control policies and evaluating the expected lifetime of power modules. We have chosen the WLTC, depicted in Figure 4, as the speed profile to assess the expected lifetime of the IGBTs in this research study. The simulation parameters are presented in Table I.

TABLE I: Simulation parameters.

Quantity	Value	Description
R_s	1 Ω	Stator resistance
Φ_M	0.03 Wb	Permanent magnet flux linkage
J	0.5 kg.m^{-2}	Rotational inertia
B_f	0.05 N.m.s	Viscous friction coefficient
L_d and L_q	10 mH	d- and q-axis inductance
p	8	Number of pole-pairs
R_θ	0.6 °C W^{-1}	Semiconductor thermal resistance
C_θ	4 N.m.K^{-1}	Semiconductor thermal capacitance
V_{ce0}	2 V	IGBT collector-emitter on-state voltage
r_{CE}	8 mΩ	IGBT On-state resistance

Figure 4 compares the performance of the two different control strategies. When employing the *Performance-Oriented* controller, the simulated speed closely matches the reference trajectory, with a minimal root mean square deviation error (RMSE) of 0.02 km/h. In contrast, the *Reliability-Aware* controller yields a higher speed tracking RMSE of 7.0 km/h, as expected.

Figure 5 illustrates the resulting current profile across the entire drive cycle, it provides a comparison between the two control strategies in terms of current, and hence temperature, fluctuation impacting the damage experienced by the converter semiconductors. Notably, the *Reliability-Aware* control strategy demonstrates reduced current fluctuations compared to the *Performance-Oriented* control. Figure 6 displays the junction temperature of a single IGBT, we can observe that the *Reliability-Aware* control policy leads to reduced temperature fluctuations. To analyse the impact on IGBT lifetime, we compute the number of temperature cycles using the Rainflow-counting algorithm, a widely employed tool in fatigue analysis.

A. IGBT lifetime analysis

The concept of linear damage accumulation, originally proposed by Palmgren and Miner [28, 29], is a well-established technique for computing the total experienced damage from the individual damage components caused by damaging cycles of different stress levels. Specifically, considering k different stress magnitudes within a spectrum S_i (where $1 \leq i \leq k$), the total number of experienced cycles for each stress level, $n_i(S_i)$, and the number of cycles to failure for each stress level $N_i(S_i)$, the overall damage is computes as follows:

$$D = \sum_{i=1}^{k} \frac{n_i(S_i)}{N_i(S_i)}. \tag{17}$$

Failure is often characterized by $D = 1$ [30].

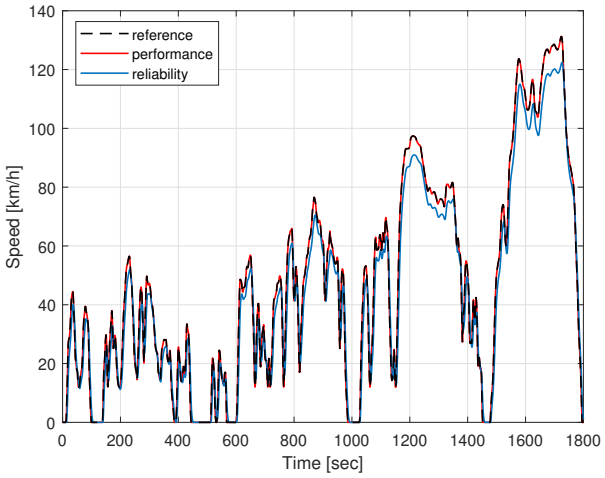

Fig. 4: Speed tracking performance for two different control policies compared to the reference WLTC drive cycle.

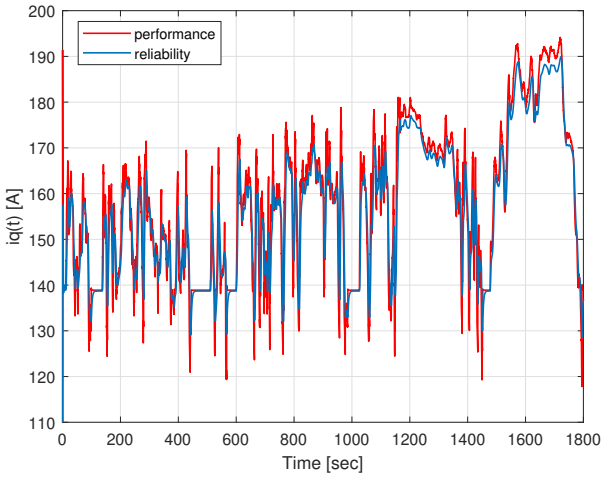

Fig. 5: Comparing the q-component of the motor current for two different control policies.

In our case, the total damage is computed as follows

$$D = \sum_{\Delta T_{\mathrm{j,min}}}^{\Delta T_{\mathrm{j,max}}} \sum_{T_{\mathrm{j,min}}}^{T_{\mathrm{j,max}}} \sum_{t_{\mathrm{on,min}}}^{t_{\mathrm{on,max}}} \frac{n(\Delta T_{\mathrm{j}}, T_{\mathrm{j}}, t_{\mathrm{on}})}{N_f(\Delta T_{\mathrm{j}}, T_{\mathrm{j}}, t_{\mathrm{on}})}, \tag{18}$$

where the number of cycles, $n(\Delta T_{\mathrm{j}}, T_{\mathrm{j}}, t_{\mathrm{on}})$, is obtained from the Rainflow-counting algorithm.

Figure 7 compares the distribution of the junction temperature cycling data obtained through the Rainflow-counting algorithm. For better comparison, the sum of cycles is computed across the cycle duration, t_{on}, to achieve $n(\Delta T_{\mathrm{j}}, T_j)$, i.e. the number of cycles for different T_j and ΔT_j. As we can see, using the *Reliability-Aware* control policy, results in a shift of thermal cycles from higher to lower junction temperatures, and in the reduction of cycles with high temperature variations.

The damage index of a single IGBT is computed based on the empirical lifetime model per Equation (12) combined

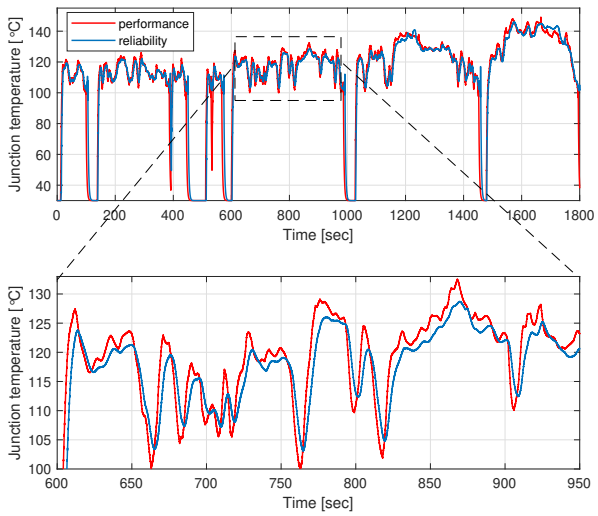

Fig. 6: Representation of the IGBT junction temperature variation, with a particular focus on relevant segments.

with the cumulative damage model in Equation (18):

$$\mathrm{D_{perf}} = 1.6 \times 10^{-4},\ \mathrm{D_{rel}} = 1.1 \times 10^{-4}.$$

As we can see, with the *Reliability-Aware* control scheme, the total damage on the IGBT is reduced by approximately 30% over the entire drive cycle of WLTC. We can conclude that, under the *Performance-Oriented* control, the IGBT is predicted to endure for approximately 6,200 drive cycles, which is equivalent to approximately 8 years, assuming that two drive cycles are completed daily (this is equivalent to 1 hour of driving per day). When *Reliability-Aware* control is used to operate the IGBT, its estimated lifetime would correspond 9,000 drive cycles, or an equivalent of 12 years. Those absolute numbers are highly dependent on the chosen drive-cycles, therefore those results have to be interpreted as relative in the context of controller performance comparison.

VI. Conclusion

Traditionally, the operation of BEVs, focuses on maximizing performance and at best efficiency. It is only recently that the engineering community is becoming aware of the importance to address sustainability objectives by designing and operating systems to maximize their lifespan and hence reduce resource waste and environmental pollution.

Within this context, this paper focuses on the concept of reliability control, where the operation of BEVs power converters is optimized to achieve the desired tracking performance while minimizing damage to the power semiconductor switches, thereby increasing the lifetime at the system level. In particular, we proposed an $\mathcal{H}_\infty$ controller to efficiently and reliably operate BEV power converters under varying driving conditions.

We provided case studies to illustrate the effectiveness of the proposed control policies in real-world scenarios, emphasizing its benefits in terms of energy efficiency and

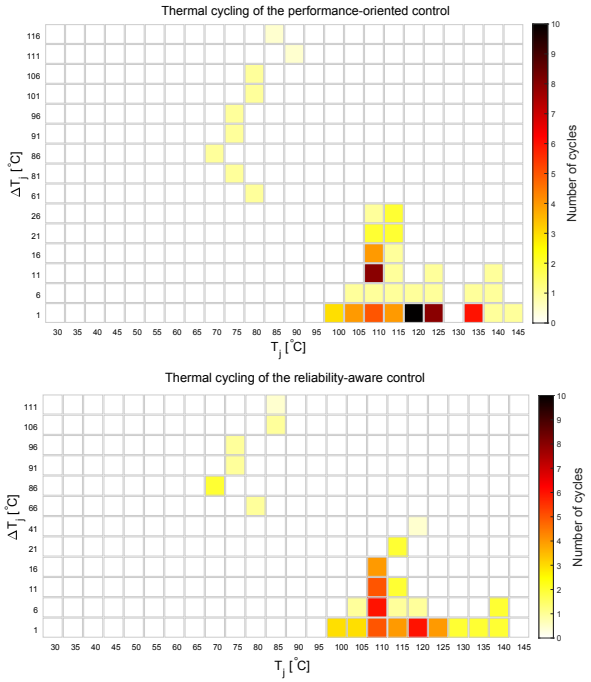

Fig. 7: The number of thermal cycles of IGBT junction temperature vs different T_j and ΔT_j. Top: performance-oriented control policy. Bottom: reliability-aware control policy.

lifetime expectations. The proposed approach offers a novel perspective and insights into the sustainable operation of BEVs, paving the way for an entire suite of studies toward a more environmentally friendly and reliable automotive future.

REFERENCES

[1] M. Fanoro, M. Božanić, and S. Sinha, "A review of the impact of battery degradation on energy management systems with a special emphasis on electric vehicles," *Energies*, vol. 15, no. 16, 2022.

[2] F. Spaven, Y. Liu, and M. Baghdadi, "Going further with smaller EVs: System-level battery range, emissions and charging infrastructure analysis," *Journal of Cleaner Production*, vol. 369, 2022.

[3] D. Pevec, J. Babic, A. Carvalho, Y. Ghiassi-Farrokhfal, W. Ketter, and V. Podobnik, "A survey-based assessment of how existing and potential electric vehicle owners perceive range anxiety," *Journal of Cleaner Production*, vol. 276, 2020.

[4] K. Sato, D. Navarro, S. Sekizaki, Y. Zoka, N. Yorino, H. J. Mattausch, and M. Miura-Mattausch, "Prediction of DC-AC converter efficiency degradation due to device aging using a compact MOSFET-aging model," *IEICE Transactions on Electronics*, vol. E103.C, no. 3, pp. 119–126, 3 2020.

[5] S. Sudhakar, V. Sze, and S. Karaman, "Data Centers on Wheels: Emissions From Computing Onboard Autonomous Vehicles," *IEEE Micro*, vol. 43, no. 1, 2023.

[6] G. Zardini, N. Lanzetti, M. Pavone, and E. Frazzoli, "Analysis and Control of Autonomous Mobility-on-Demand Systems," *Annual Review of Control, Robotics, and Autonomous Systems*, vol. 5, no. 1, pp. 633–658, 6 2022.

[7] J. Zhang, T. Liu, and J. Qiao, "Solving a reliability-performance balancing problem for control systems with degrading actuators under model predictive control framework," *Journal of the Franklin Institute*, vol. 359, p. 9, 2022.

[8] T. Meyer, "Optimization-based reliability control of mechatronic systems," Ph.D. dissertation, 12 2016.

[9] K. Sayed, A. Almutairi, N. Albagami, O. Alrumayh, A. G. Abo-Khalil, and H. Saleeb, "A review of dc-ac converters for electric vehicle applications," *Energies*, vol. 15, no. 3, 2022.

[10] S. Surya, S. P, and S. S. Williamson, "A Comprehensive Study on DC–DC and DC–AC Converters in Electric and Hybrid Electric Vehicles," in *EAI/Springer Innovations in Communication and Computing*, 2022.

[11] Phillip T. Krein, *Elements of Power Electronics*. Oxford University Press, 1 2015.

[12] Q. Tang, X. Shu, G. Zhu, J. Wang, and H. Yang, "Reliability study of bev powertrain system and its components—a case study," *Processes*, vol. 9, no. 5, 2021.

[13] S. Rahimpour, H. Tarzamni, N. V. Kurdkandi, O. Husev, D. Vinnikov, and F. Tahami, "An overview of lifetime management of power electronic converters," *IEEE Access*, vol. 10, pp. 109 688–109 711, 2022.

[14] P. D. Reigosa, H. Wang, Y. Yang, and F. Blaabjerg, "Prediction of bond wire fatigue of igbts in a pv inverter under a long-term operation," *IEEE Transactions on Power Electronics*, vol. 31, no. 10, pp. 7171–7182, 2016.

[15] M. H. Nguyen and S. Kwak, "Enhance reliability of semiconductor devices in power converters," *Electronics*, vol. 9, no. 12, 2020.

[16] H. Wang, M. Liserre, F. Blaabjerg, P. de Place Rimmen, J. B. Jacobsen, T. Kvisgaard, and J. Landkildehus, "Transitioning to physics-of-failure as a reliability driver in power electronics," *IEEE Journal of Emerging and Selected Topics in Power Electronics*, vol. 2, no. 1, pp. 97–114, 2014.

[17] M. Ciappa and W. Fichtner, "Lifetime prediction of igbt modules for traction applications," in *2000 IEEE International Reliability Physics Symposium Proceedings. 38th Annual (Cat. No.00CH37059)*, 2000, pp. 210–216.

[18] W. Wu, G. Gao, L. Dong, Z. Wang, M. Held, P. Jacob, and P. Scacco, "Thermal reliability of power insulated gate bipolar transistor (igbt) modules," in *Twelfth Annual IEEE Semiconductor Thermal Measurement and Management Symposium. Proceedings*, 1996, pp. 136–141.

[19] P. C. Krause, O. Wasynczuk, S. D. Sudhoff, and S. Pekarek, *Analysis of electric machinery and drive systems*. Wiley Online Library, 2002, vol. 2.

[20] Q. Huang, Q. Huang, H. Guo, and J. Cao, "Design and research of permanent magnet synchronous motor controller for electric vehicle," *Energy Science & Engineering*, vol. 11, no. 1, pp. 112–126, 2023.

[21] X. Liu, H. Chen, J. Zhao, and A. Belahcen, "Research on the performances and parameters of interior pmsm used for electric vehicles," *IEEE Transactions on Industrial Electronics*, vol. 63, no. 6, pp. 3533–3545, 2016.

[22] Y. Zhang, W. Cao, S. McLoone, and J. Morrow, "Design and flux-weakening control of an interior permanent magnet synchronous motor for electric vehicles," *IEEE Transactions on Applied Superconductivity*, vol. 26, no. 7, pp. 1–6, 2016.

[23] T. Koottungal, P. Reigosa, S. Mitrova, M. Rahimo, R. A. Minamisawa, and S. Mastellone, "Reliability study of an adjustable hybrid switch (ahs) for a high power automotive converter," *submitted to IEEE Journal of Emerging and Selected Topics in Power Electronics*, 2023.

[24] L. Sandel, G. Zardini, S. Mitrova, T. Thekemuriyil, R. Minamisawa, M. Rahimo, A. Censi, E. Frazzoli, and S. Mastellone, "Enhancing efficiency and reliability of electric vehicles via adaptive e-gear control," in *2023 IEEE International Intelligent Transportation Systems Conference (ITSC)*, 2023.

[25] U. D. of Defense, Ed., *The Military Handbook for Reliability Prediction of Electronic Equipment MIL-HDBK-217F*. Defense Printing Service, 1995.

[26] A. Wintrich and U. Scheuermann, "Power cycle model for IGBT product lines," Semikron Danfoss, Nuremberg, Germany, Application Note AN21-001, 2021.

[27] N. Mohan, T. M. Undeland, and W. P. Robbins, *Power Electronics. Converters, Applications and Design*, 3rd ed. John Wiley and Sons, Inc, 2003.

[28] A. Czechowski and A. Lenk, "Miner's rule in mechanical tests of electronic parts," *IEEE Transactions on Reliability*, vol. R-27, no. 3, pp. 183–190, 1978.

[29] M. A. Miner, "Cumulative damage in fatigue," *Journal of Applied Mechanics*, vol. 12, no. 3, pp. A159–A164, 1945.

[30] J. Slavič, M. Boltezar, M. Mrsnik, M. Cesnik, and J. Javh, *Vibration Fatigue by Spectral Methods: From Structural Dynamics to Fatigue Damage–Theory and Experiments*. Elsevier, 2020.